J Sol-Gel Sci Technol (2016) 79:249–261
DOI 10.1007/s10971-015-3920-0

ORIGINAL PAPER: SOL-GEL, HYBRIDS AND SOLUTION CHEMISTRIES

Heterobimetallic sol–gel precursors and intermediates

Ulrich Schubert[1]

Received: 14 September 2015 / Accepted: 17 November 2015 / Published online: 15 December 2015

Abstract The question how the metals in bimetallic sol–gel materials are positioned relative to each other and how the dispersion of the metals can be controlled is a major preparative and analytical challenge. Two particular aspects are addressed: The first is an alternative type of single-source precursors where the two metals are interlinked through an organic spacer. The new options provided by this approach are demonstrated for metal oxide/silica nanocomposites, zinc titanate and Co_3O_4/ceria catalysts. The second issue with regard to heterobimetallic systems is the kind of intermediates formed during sol–gel co-processing of two different metal precursors (metal alkoxides or metal alkoxide + metal salt). Systematic investigation of the structures of Ti/M oxo clusters (M = main group or transition metal, or lanthanide) shows some interesting common construction principles and thus sheds light on early stages of the structural evolution in mixed-metal oxide systems.

Graphical abstract

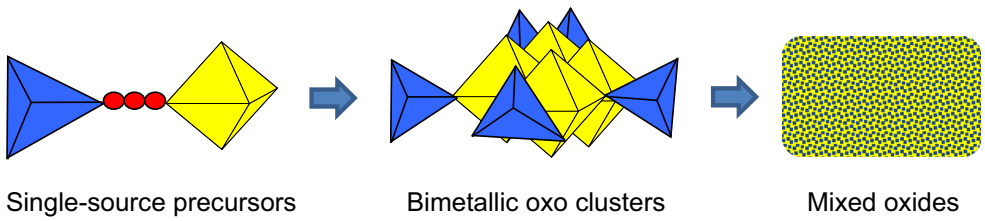

Keywords Single-source precursors · Titanium alkoxides · Sol–gel method · Metal oxo clusters

1 Introduction

Preparation of bi- or multimetallic oxide materials by classical routes, such as solid-state reactions, results in compounds with fixed metal ratios and equilibrium structures, corresponding to the respective phase diagrams. During sol–gel processing [1], however, oxidic materials formed in kinetically controlled reactions. The initially obtained solids (amorphous, nanocrystalline, etc.) remain in the state of thermodynamic non-equilibrium as long as the materials are not exposed to temperatures at which crystallization (or extensive crystal growth) sets in. The fact that (oxide-based) gels are far away from thermodynamic equilibrium allows, among others, preparing organic–inorganic hybrid materials, but also mixed-metal materials with, in principle, any ratio of the corresponding metals (without the limitations of phase diagrams).

Kinetically controlled multicomponent reactions, however, entail a major obstacle, which is control of the homogeneity of the produced materials. This is due to the different reaction rates of the precursor compounds and

✉ Ulrich Schubert
Ulrich.Schubert@tuwien.ac.at

[1] Institute of Materials Chemistry, Vienna University of Technology, Getreidemarkt 9, 1060 Vienna, Austria

intermediates. "Homogeneity" is a question of length scale. Materials may appear homogeneous to the naked eye, despite being in fact inhomogeneous on, for example, the nanometer scale. A random distribution of the building blocks in sol–gel materials could only be expected if the reaction rates of all components would be the same, which is very unlikely.

This article, which is to a large extent an account of own work, addresses two particular aspects of bimetallic sol–gel materials. The first is an alternative type of single-source precursors (SSP) which opens up new options for controlling the metal dispersion in bimetallic oxides. The second tries to shed some light on early stages of the structural evolution of mixed-metal oxide gels prepared from either two metal alkoxides or a metal alkoxide and a metal salt.

2 A new type of single-source precursors

Mixed-metal oxide materials can be prepared by sol–gel processing through several approaches. The most common is the use of precursor mixtures, where several strategies have been developed to avoid macroscopic phase separation, such as pre-hydrolysis of the faster-reacting component or use of chemical additives. In the latter, the relative reactivity of the precursors is adjusted by chemical modification. Another method is impregnation of pre-formed gels by a second component (an example will be given later in this article). These methods have in common that the dispersion of the metals can hardly be controlled in a rational manner, especially on a nanometer scale, although *macroscopical* homogeneous materials may be obtained. These methods will not be discussed here; they have been accounted for in detail in review articles and textbooks on sol–gel processing.

Non-hydrolytic sol–gel processes have been used for the preparation of mixed-metal oxides, starting from mixtures of metal alkoxides and (mostly) metal halides [2]. The oxo groups are formed by RCl elimination between a M-Cl and a M′-OR group. This leads to a very good control over the distribution of the elements in mixed-oxide systems. There are limitations, however, with regard to the choice of metals and the M/M′ ratio.

Single-source precursors for sol–gel processing until present are nearly exclusively alkoxo(or diolate)-bridged compounds [3, 4]. Although some of them were successfully converted to mixed-oxide materials, they have not made a breakthrough, and the level of homogeneity of the obtained oxides was not investigated in most cases. The underlying chemical issue is that alkoxo-bridged (heterometallic) dimers or oligomers are in equilibrium with the corresponding monomeric species which have a different reactivity. It is therefore not apparent which species actually react during sol–gel processing (i.e., whether alkoxo-bridged SSPs react differently to mixtures of metal alkoxides) and whether the connectivity of the metals is retained.

We therefore propose an alternative approach to connect the metals in SSPs through bifunctional organic groups instead of alkoxo (or diolate) bridges. This approach goes back to a method of preparing metal oxide/silica nanocomposites we had developed in the early 1990s [5, 6]. An example is shown in Fig. 1 [7]. Dispersion of the metals is controlled by tethering the metal ions to the $Si(OR)_3$ entities by means of an organic spacer. To this end, organically substituted alkoxysilanes of the type $(RO)_3Si(CH_2)_nX$ are used, where X is a coordinating group. Some examples are shown in Fig. 2 [8–10]. Metal complexes $[(RO)_3Si(CH_2)_nX]_mM^{x+}$ are formed in situ, i.e., the two-component system (an alkoxysilane and a metal compound) is transformed in a SSP. Metal coordination is retained during sol–gel processing, as can be shown by UV spectroscopy. The metal proportion in the composite can be adjusted by co-processing of $[(RO)_3Si(CH_2)_nX]_mM^{x+}$ with $Si(OR)_4$. High—ideally a molecular—dispersion is thus achieved. Nanocomposites, i.e., non-agglomerated, monodispersed nanometer-sized metal oxide particles dispersed in silica, are then obtained by controlled (mostly thermal) degradation of the organic tethers in a subsequent (calcination) step. The diameter of the metal oxide nanoparticles mainly depends on the kind of metal and its counter-ion, the kind of the complexing silane and the reaction conditions during the removal of the organic groups [7, 11]. The fact that metal oxide/silica nanocomposites composites are formed rather than metal silicates is due to the relatively low temperatures during calcination. An example for the other possibility will be given later in this article.

Metal/SiO_2 composites can be obtained by reduction of the metal oxide particles in a hydrogen atmosphere, but other chemical transformations of the originally obtained metal oxide nanoparticles are also possible. For example, metal nitride/SiO_2 nanocomposites were prepared by high-temperature treatment of the metal oxide/SiO_2 composites with ammonia [12] and a few metal sulfide/SiO_2 nanocomposites by treatment of the latter with ammonium sulfide solution [13].

Not only single metal ions can be tethered to amino-substituted trialkoxysilanes, but also oligomeric inorganic structures. The cyanometallate $[Ni(AEAPTS)_2]_3[Fe(CN)_6]_2$ (AEAPTS = $(MeO)_3SiCH_2CH_2CH_2NHCH_2CH_2NH_2$) was prepared by treatment of $[Ni(AEAPTS)_2]Cl_2$ with $K_3[Fe(CN)_6]$ (Fig. 3). AEAPTS acts as both a blocking ligand at Ni^{2+} and links the cyanometallate structure to silica through reaction of the trialkoxysilyl groups.

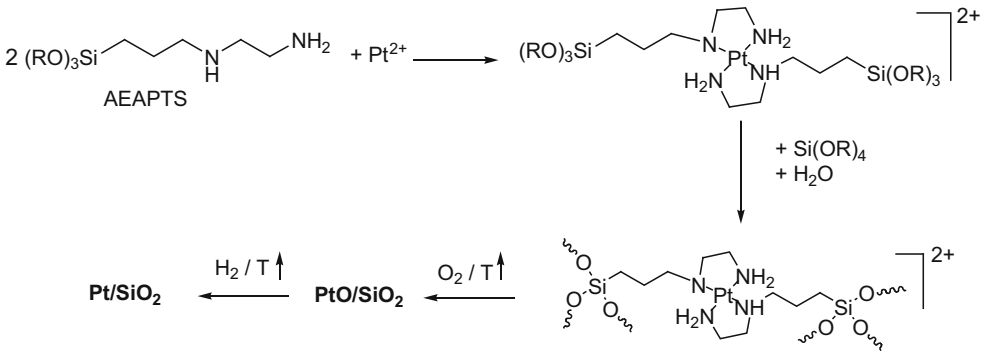

Fig. 1 Preparation of Pt/SiO_2 composites by means of the ethylene diamine-substituted silane AEAPTS

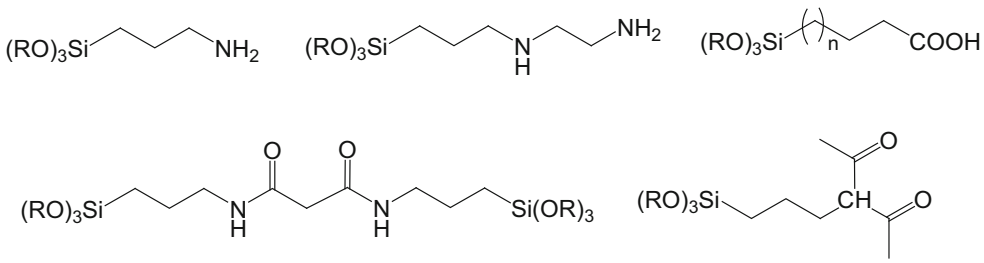

Fig. 2 Selection of silanes $(RO)_3Si(CH_2)_nX$, where X is a functional group capable of coordinating metal ions or metal compounds

Cyanometallates often have interesting magnetic properties because the M–N≡C–M′ bridges enable magnetic coupling between the transition metals. SQUID measurements showed that the material obtained by sol–gel processing of $[Ni(AEAPTS)_2]_3[Fe(CN)_6]_2$ exhibits magnetic ordering below 22 K with an effective magnetic moment μ_{eff} of 4.46 μ_B at room temperature and a maximum of 8.60 μ_B at ~15 K. Fe–C≡N–Ni structures are retained in the gel (otherwise the materials would not be ferromagnetic) although the structure of the cyanometallate moieties in the gel is probably different to that of the parent compound [14].

Late transition metal ions (M^{m+}) form a variety of amine complexes, and therefore amino-substituted silanes (as in Fig. 2) can be used for the formation of SSPs $[(RO)_nSi(CH_2)_mNR_2]_nM^{x+}$. Although early transition metal alkoxides form amine adducts, such as $[Ti(OR)_4(NHR_2)]_2$ [15, 16], such complexes are not stable enough for sol–gel processing. Therefore other functionalities must to be employed for the formation of SSPs of early transition (and main group) metals. Metal alkoxides, $M(OR)_n$, are well known to react with a variety of protic compounds with bi- or tridentate anions (BL-H), such as β-diketones, carboxylic or phosphonic acids, oximes or aminoalcohols, to give derivatives of the type $M(OR)_{n-x}(BL)_x$ [17]. The $Si(OR)_3$-substituted β-diketone $(MeO)_3Si(CH_2)_3CH(CMe{=}O)_2^8$ (OTH-H, see Fig. 2) [8] was used for reactions with metal alkoxides, such as $Ti(OR)_4$, $Zr(OR)_4$ or $Al(OR)_3$, to give a SSP where two hydrolyzable moieties are connected with each other, viz. $Si(OR)_3$ and $M(OR)_{n-1}$ (Fig. 4) [18]. A related SSP was recently prepared by reaction of $(MeO)_3Si(CH_2)_mCOOH$ (see Fig. 2) with $Ti(OR)_4$ [10].

Transparent, macroscopically homogeneous gels were obtained upon sol–gel processing of $M(OR)_x(OTH)$ ($M(OR)_x$ = $Ti(OiPr)_3$, $Al(OsBu)_2$) [18]. Contrary to this, immediate precipitation of titania gel occurs when water is added to a solution containing both $Si(OR)_4$ and $Ti(OR)_4$, because of the much higher reactivity of $Ti(OR)_4$ toward water. Thus, a *macroscopic* phase separation is avoided by the organic link between the $Si(OMe)_3$ and the $Ti(OiPr)_x$ group, resulting in a controllable gelation behavior. In passing, this is similar to organic co-polymers. Macroscopic phase separation may occur in mixtures of two polymers with different polarity. In contrast, when segments of the two polymers are linked to each other, i.e., in diblock co-polymers, only nanosized domains can form.

SAXS investigations through all preparation stages, i.e., hydrolysis of $M(OR)_x(OTH)$, gelation, aging and drying, resulted in a clear picture on the structure evolution [19, 20]. Small MO_x particles (clusters) are formed immediately after addition of water. Their size ($r = 0.5 \pm 0.1$ nm for M = Ti and 0.7 ± 0.1 nm for M = Al) remains constant through gelation and aging. The MO_x clusters probably cannot grow, because they are covered by a $(OCMe)_2C-(CH_2)_3Si(OMe)_3$ shell (Fig. 5). An interesting side aspect is that the size of these MO_x clusters is in the same range as that of isolated and structurally characterized molecular clusters of the type $M_aO_b(OR/OH)_c(BL)_d$ (BL = bidentate ligands, mostly carboxylates) (see below) [21]. The

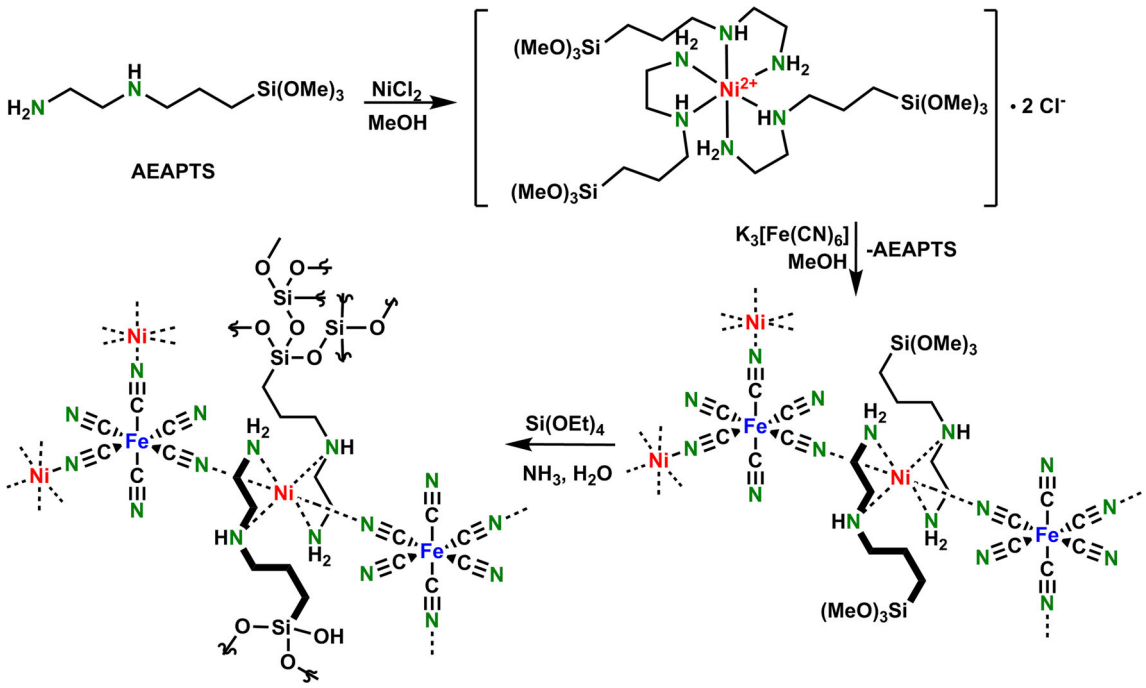

Fig. 3 Synthesis sequence from $[Ni(AEAPTS)_3]^{2+}$ through the cyanometallate network to the final sol–gel material. The *trans* arrangement of the CN groups at Ni was drawn only for graphical reasons

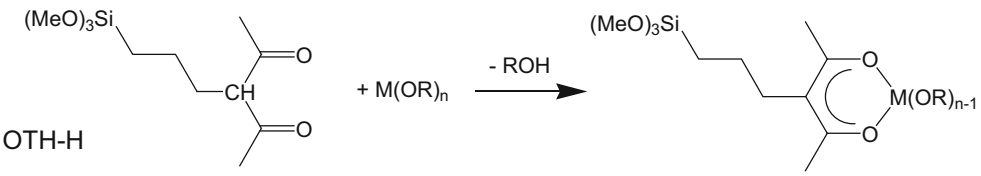

Fig. 4 Synthesis of single-source precursors (SSP) by means of the β-diketone-substituted silane OTH-H

condensation reaction then proceeds by the slower hydrolysis and condensation of the $Si(OMe)_3$ groups, i.e., a silica matrix is formed around the MO_x clusters. When $M(OR)_x(OTH)$ is co-reacted with $Si(OEt)_4$, the additional Si/O is incorporated between the clusters, i.e., dilutes the MO_x clusters in the silica network. MO_x nanoparticles (titania, zirconia, alumina) in silica are formed when the organic groups tethering Si and M (M = Ti, Zr, Al) during sol–gel processing are degraded by heating the xerogels in air to 500–600 °C [18].

A variety of alkoxysilanes $(RO)_3Si–Y–X$ with coordinating groups X and inert spacers Y (mostly $(CH_2)_m$) is available, and SSPs $[(RO)_3Si–Y–X]_nM^{x+}$ are easily obtained as discussed before. A generalization of this method for the preparation of mixed oxides of any two metallic elements is less straightforward. It requires bifunctional organic compounds X′–Y–X with two different coordinating groups (X and X′) where each of them must selectively react with just one metal (M and M′ = metal ions, $M(OR)_x$ groups, or similar). This would lead to SSPs of the type M′(X′–Y–X)M. Coordination of both groups (X and X′) to the same metal (leading to coordination polymers or chelated complexes) must be avoided. Suitable groups X and X′ are those which have been used for the organic modification of metal alkoxides. They are typically bidentate (or multidentate) ligands, such as carboxylates, β-diketonates, β-ketoesters, aminoalcoholates, oximates, α-amino- or hydroxycarboxylates, phosphonates, phosphinates or sulfonates. The chemistry of organically modified metal alkoxides is sufficiently well understood, [17] including a qualitative assessment of the bond strength of a particular group to a particular metal. The most suitable choice of X and X′ for the preparation of M′(X′–Y–X)M SSPs depends of course on the metals M and M′ and must be deliberately chosen for each metal combination.

Two cases will be discussed in the following, where *p*-carboxybenzaldehyde oxime (POBC-H) proved to be a suitable molecule of the type X′–Y–X. Reaction of POBC-H with zinc acetate led to the formation of $Zn(OOC\text{-}C_6H_4\text{-}CH{=}NOH)_2$, i.e., the carboxylate groups were selectively coordinated to Zn^{2+} [22]. The dangling oxime groups were

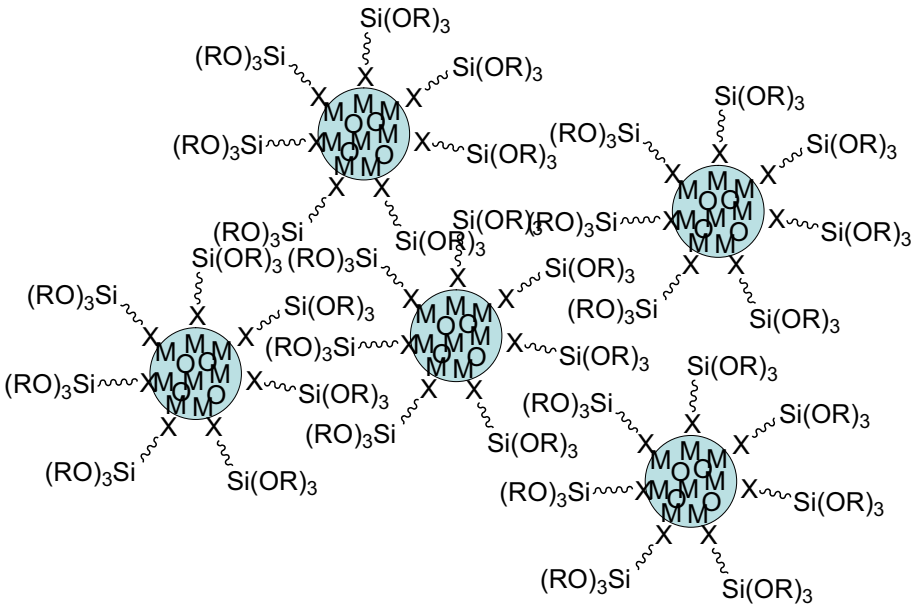

Fig. 5 Schematic representation of the early stage of $(MeO)_3Si(CH_2)_3C(CMe{=}O)_2[M(OR)_x]$ hydrolysis, where small M/O primary particles (M = Al, Ti, Zr) are formed

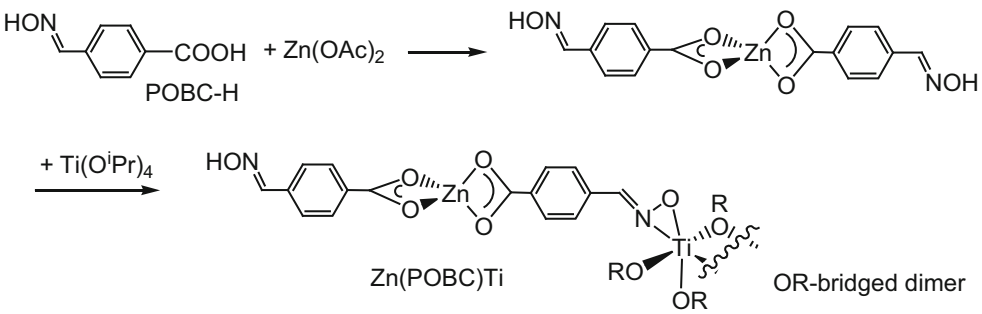

Fig. 6 Preparation of a Zn/Ti SSP with *p*-carboxybenzaldehyde oxime (POBC) as organic linker (dimerization of the $Ti(OR)_3$ moieties through OR bridges is not relevant for subsequent sol–gel processing)

subsequently reacted with one equivalent of $Ti(O\mathit{i}Pr)_4$, resulting in the SSP shown in Fig. 6 (Zn(POBC)Ti) [23]. Both steps can be easily monitored by ^{1}H NMR spectroscopy: the COOH signal disappears in the first step, and the NOH signal is weakened in the second step. (When $Zn(OOC\text{-}C_6H_4\text{-}CH{=}NOH)_2$ is reacted with an excess of $Ti(O\mathit{i}Pr)_4$, the NOH signal disappears completely because the terminal NOH groups also react and a coordination polymer with a Zn/Ti ratio of 1:2 is formed).

Sol–gel processing of the Zn(POBC)Ti SSP was compared with that of a mixture of two individual precursors (zinc benzoate + acetaldoximate-modified $Ti(O\mathit{i}Pr)_4$ [Zn-BA/Ti-AO]). Benzoic acid and acetaldoxime were chosen as modifying agents to ensure similar electronic properties (and thus reactivity) of the two metals compared to Zn(POBC)Ti. The sol obtained from the SSP had an orange color (Fig. 7a) and was stable for weeks, while that of Zn-BA/Ti-AO was turbid (Fig. 7b). The appearance of the two sols, prepared under the same conditions, already indicated that the sol derived from the SSP was more homogeneous.

After sol–gel processing, the gels were calcined in air to remove the organic groups. In situ SAXS measurements were performed in order to follow the structural changes during heating [23]. Only one peak was observed in the whole temperature range for Zn(POBC)Ti (Fig. 7c). In contrast, Zn-BA/Ti-AO showed one broad short-range-order peak only up to 200 °C. Above this temperature, two additional scattering peaks occurred, which can be interpreted as a phase separation into regions with different composition (Fig. 7d). Regions with different compositions are possibly more easily formed in Zn-BA/Ti-AO due to the lack of connection between the zinc and titanium moiety. Thus, the hybrid material prepared from the SSP retains a more homogeneous structure once the organic groups start to degrade. The structural differences between the two types of samples become blurred above 400 °C

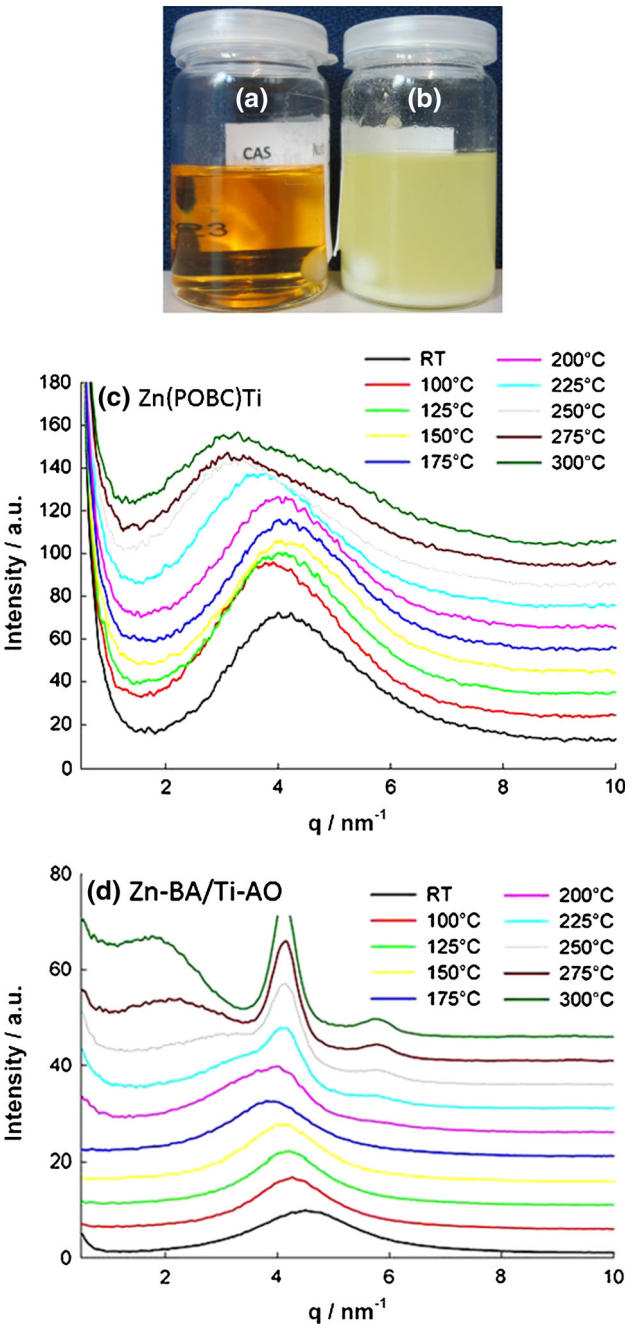

Fig. 7 Zn–Ti sols from **a** Zn-POBC-Ti and **b** [zinc benzoate + oximate-modified $Ti(OiPr)_4$]. In situ SAXS measurement of **c** Zn-POBC-Ti and **d** Zn-BA/Ti-AO from 100 to 300 °C in 25 °C steps (*RT* room temperature), with a heating rate of 5 °C/min between the measurement intervals. Reproduced from Ref. [23] with permission from The Royal Society of Chemistry

after complete removal of all organic groups, i.e., in the temperature regime of "normal" solid-state reactions, where $ZnTiO_3$ crystallites start to be formed. The use of the SSP is therefore beneficial for obtaining homogeneous structures in the gel stage, it simplifies the preparation protocol if the SSP is prepared in situ, and it allows a more controlled synthesis of the mixed oxide.

A second example where homogeneous mixed-metal oxides were obtained by means of a POBC-based SSP is Co_3O_4–CeO_2 composites, which are interesting CO oxidation catalysts [24]. A composite is formed because no ternary oxide is known for this metal combination (as in the case of $ZnTiO_3$) and only 5 % Co can be incorporated into the CeO_2 lattice [25]. The SSP Co(POBC)Ce was prepared by reaction of $Co(OAc)_2$ with POBC-H (where again only the carboxylate groups of POBC-H react with the Co^{2+} ions), followed by in situ reaction of the formed $Co(POBC)_2$ with an excess of $Ce(OtBu)_4$ (Co/Ce = 1:4) (Fig. 8).

For comparison, two other variations of sol–gel processing were chosen, differing by the way of introducing Co^{2+} ions into the gels (Fig. 9) [24]. After sol–gel processing, all gels were solvothermally treated in ethanol followed by heat treatment in air at 500 °C to remove the organic groups. In route 1, a ceria gel was synthesized first from $Ce(OtBu)_4$, and $Co(OAc)_2$ was then added to the gel. In route 2, a mixture of $Ce(OtBu)_4$ and $Co(OAc)_2$ was subjected to sol–gel processing. In route 3, only the SSP Co(POBC)Ce was employed. The way by which Co was introduced clearly influenced the morphology of the composites on the nanoscale. Using the SSP Co(POBC)Ce (route 3) resulted in a very homogeneous dispersion of Co oxide in the ceria matrix (Fig. 9, right image), as was expected from the previous results. When a pre-formed ceria gel was impregnated with $Co(OAc)_2$ (route 1), Co_3O_4 particles were located on the surface of CeO_2 particles or agglomerates thereof (Fig. 9, left image). Sol–gel co-processing of $Ce(OtBu)_4$ and $Co(OAc)_2$ (route 2) resulted in an intimate mixture of CeO_2 and Co_3O_4 particles (Fig. 9, center). The results clearly show that these variations of the synthesis route resulted in three different morphologies on the nanoscale, despite the same Co/Ce ratio, the same metal precursors and the same processing steps (sol–gel processing + solvothermal treatment). The use of the SSP resulted in the most homogeneous dispersion of Co in ceria.

3 Mixed-metal oxo clusters

Amorphous solids, by definition, do not have structures with regularly repeating arrangements of atoms. It is well known from glass science, however, that the non-periodic arrangement of the primary units, such as $[SiO_4]$ tetrahedra, does not exclude the presence of structural sub-units, such as boroxol rings in borate glasses or spherosilicate units in silicate glasses. While structural features of amorphous solids larger than a few nanometers can be investigated by TEM or SAXS, for example, there is hardly any method for obtaining structural information on an atomic scale.

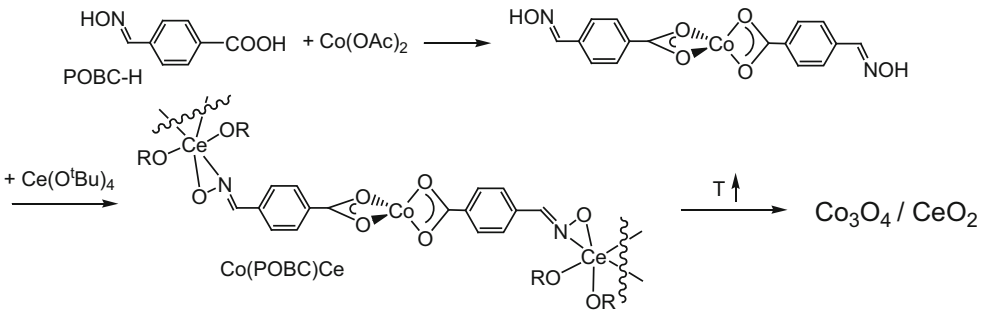

Fig. 8 Preparation of Co_3O_4–CeO_2 nanocomposites by using the SSP Co-POBC-Ce

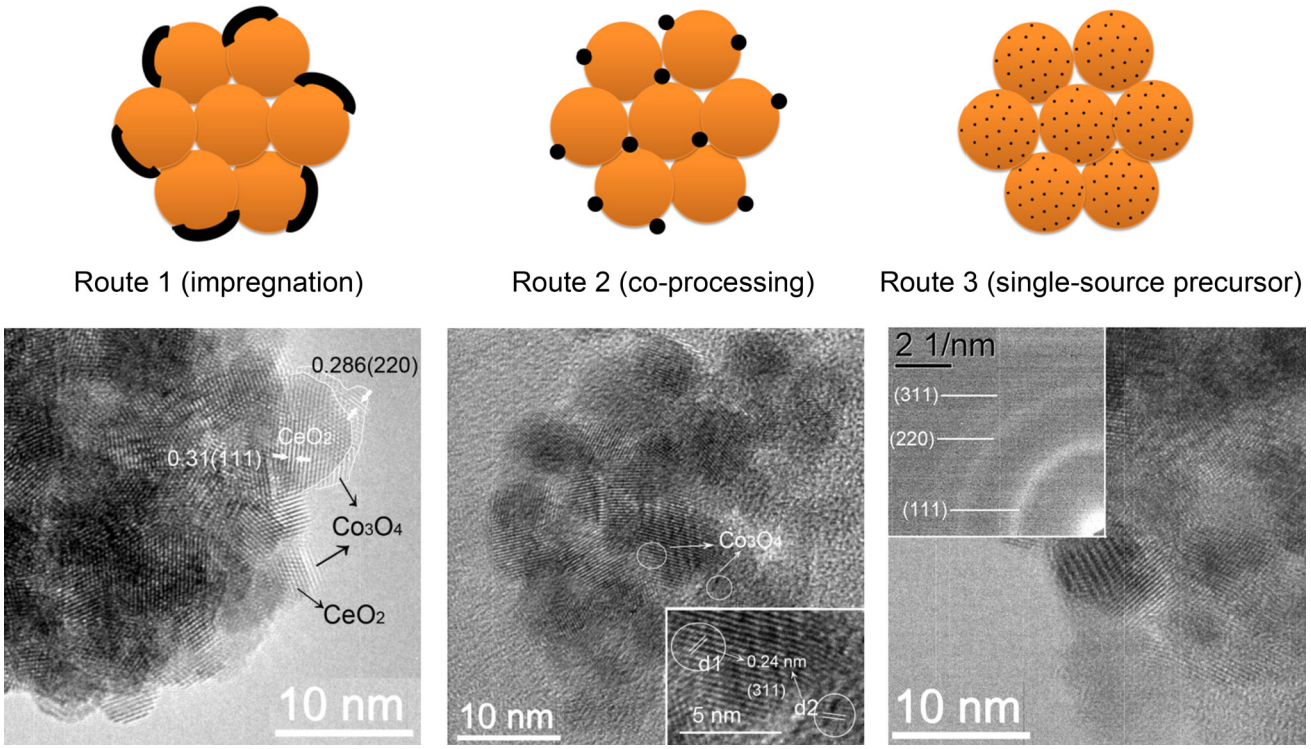

Fig. 9 Suggested morphologies and HRTEM images of the Co_3O_4–CeO_2 composites prepared by three different sol–gel routes. (*orange* CeO_2, *black* Co_3O_4)) (from Ref. [24])

Indirect evidence on structural units in oxide gels, however, can be gained from molecular compounds obtained by incomplete hydrolysis or condensation of sol–gel precursors. Much work was devoted to this issue in silicon chemistry. Early work had already provided evidence that hydrolysis and condensation of $Si(OR)_4$ or $RSiX_3$ (X = Cl, OR) proceeds through polynuclear siloxane rings and cages (Refs. [26–28] as arbitrarily selected examples).

Similar systematic work on metal alkoxides is scarce. W. G. Klemperer compiled a series of molecular clusters $Ti_aO_b(OH/OR)_c$, with nuclearities (index a) ranging from 3 to 18 (a few more were isolated later) from partially hydrolyzed titanium alkoxides [29, 30] and showed how the structures depend on the Ti/O ratio (a:b), i.e., the degree of condensation. Modification of $Ti(OR)_4$ by bidentate ligands (BL) adds a second dimension, because the structures of the clusters $Ti_aO_b(OR/OH)_c(BL)_d$ not only depend on the Ti/O (a/b) but also on the Ti/BL (a/d) ratio [21]. Each of these structures can be viewed as a snapshot of the structural development of—in this case—Ti/O structures as condensation reactions progress. For the time being, it cannot be proven whether these very structures are retained in the final gels, but this is very likely. From the collection of structures, it is obvious that some structural elements, such as $Ti_3(\mu_3\text{-}O)$ units and building blocks based thereon, develop very early during the hydrolysis and condensation process. Another indication that molecular clusters might

be building blocks for gel structures is that Ti/O units of the same size were found by SAXS measurements in the SSP-based syntheses of SiO_2/TiO_2 and $ZnTiO_3$ in the gel stage, as discussed above [19, 24].

Bimetallic systems have a third structural dimension, because the structures are not only influenced by the Ti/O and Ti/BL ratio, but additionally by the Ti/M ratio (or generally by the M/M′ ratio). The likelihood is high that bimetallic oxo clusters (=partially hydrolyzed systems) represent structural units of the final gels if the two metals are bridged by organic groups. A few mixed-metal oxo clusters with stabilizing bidentate ligands were characterized before [31, 32]. In this article, only some systematic structural investigations in our laboratories on titanium-based systems will be summarized.

Two general remarks before discussing some structural trends in Ti/M bimetallic oxo clusters:

1. Oxo clusters of the general composition $M_aO_b(OH/OR)_c(OOCR')_d$ are obtained when early transition metal alkoxides, $M(OR)_n$, are reacted with more than one molar equivalent of a carboxylic acid [21]. The carboxylic acid not only provides carboxylate ligands but also the oxo groups through esterification with the eliminated alcohol. Although such clusters can also be obtained by controlled addition of "external" water, reaction of metal alkoxides with carboxylic acids is a very easy method due to the slow in situ generation of water devoid of mixing problems.
2. Most of the clusters we have prepared are stabilized by methacrylate (OMc) ligands. Methacrylic acid was initially used for the preparation of inorganic–organic hybrid materials by free radical polymerization of the clusters with organic co-monomers [33]. It turned out that methacrylate ligands are especially well suited to get crystalline oxo clusters. The reason for this is unknown.

The most straightforward variation of the [$Ti(OR)_4$ + carboxylic acid] system is to add another four-valent metal alkoxide, such as $Zr(OR)_4$ or $Hf(OR)_4$, to the reaction mixture. Two series of structures were found, depending on the employed stoichiometric ratios and the kind of acid.

In the first series, rod-shaped structures were found (Fig. 10) [34], which consist of condensed [TiO_6] and [ZrO_8]/[ZrO_7] polyhedra. There is a tendency for the [ZrO_8]/[ZrO_7] polyhedra to condense with each other, i.e., to form the rod-like backbone, while the [TiO_6] octahedra terminate the chains or decorate the side walls. Given the similarity of Zr and Hf, it is not surprising that the same structure types were found for Ti/Zr and Ti/Zr/Hf oxo clusters [35].

At this point, the question arises whether it is possible to extend the zigzag chains observed in these clusters by insertion of additional [ZrO_7] or [ZrO_8] polyhedra, i.e., whether extended chain-like structures can be expected in TiO_2/ZrO_2 gels stabilized by organic groups.

To this end, it is worthwhile to consider the question which clusters are possible in general. Clusters are

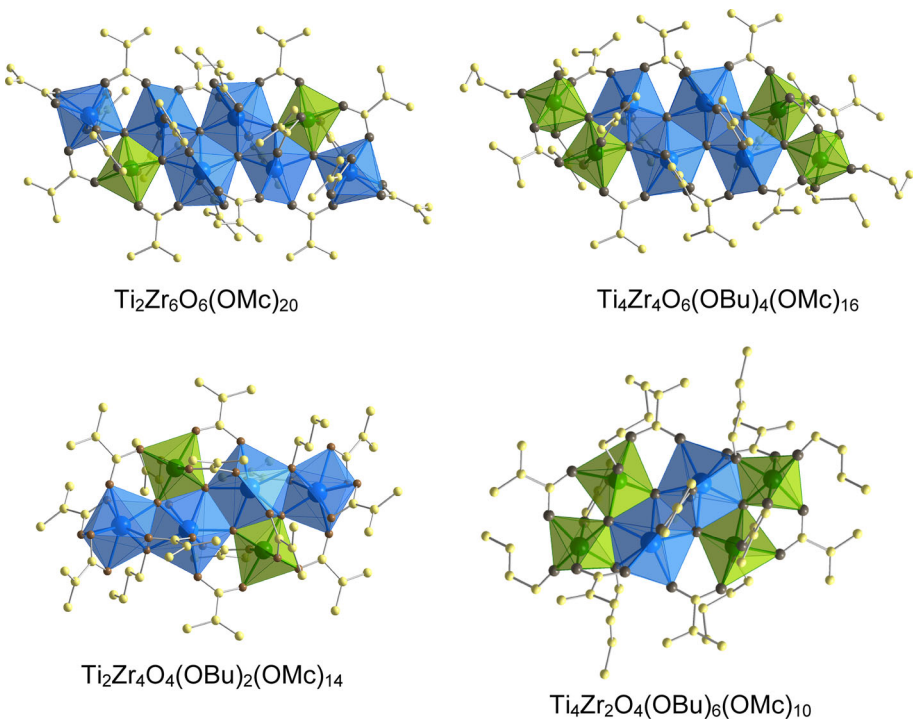

Fig. 10 Structures of $Ti_2Zr_6O_6(OMc)_{20}$, $Ti_4Zr_4O_6(OBu)_4(OMc)_{16}$, $Ti_2Zr_4O_4(OBu)_2(OMc)_{14}$ and $Ti_4Zr_2O_4(OBu)_6(OMc)_{10}$, emphasizing the coordination polyhedra of Ti and Zr

stable when both the charges and coordination numbers of the metals are balanced by the sum of the ligands. For example, both $Ti_2Zr_6O_6(OMc)_{20}$ and $Ti_4Zr_4O_6(OBu)_4(OMc)_{16}$ have the composition $M_8O_6X_{20}$ (M = Ti, Zr; X = mono-anionic ligand). The sum of the metal charges is 32 in both cases and is balanced by six O^{2-} and 20 mono-anionic ligands. The number of coordination sites, however, is different, because Ti is 6-coordinate and Zr is 7- (two Zr atoms each) or 8-coordinate. Since all oxo groups are μ_3 (thus occupying 18 coordination sites), 40 coordination sites in $Ti_2Zr_6O_6(OMc)_{20}$ and 36 in $Ti_4Zr_4O_6(OBu)_4(OMc)_{16}$ have to be filled by the alkoxo and (bidentate) carboxylate ligands. The bidentate methacrylate ligands in $Ti_2Zr_6O_6(OMc)_{20}$ occupy all coordination sites, while 4 monodentate ligands (OR) and 16 bidentate ligands (carboxylate) are needed in $Ti_4Zr_4O_6(OBu)_4(OMc)_{16}$. This calculation also explains why two zirconium atoms in $Ti_2Zr_6O_6(OMc)_{20}$ must be 7-coordinate: The additional ligands required for 8-coordination could not be compensated by the charge of the cluster core.

Coming back to the question of extended chains in such clusters: If, for example, two additional $[ZrO_7]$ or $[ZrO_8]$ polyhedra were inserted in the $Ti_2Zr_6O_6(OMc)_{20}$ cluster core, the composition of the resulting cluster would be $Ti_2Zr_8O_8X_{24}$. The mono-anionic ligands X must then occupy 52 coordination sites (for 8-coordinate Zr). Even if some of the zirconium atoms would only be 7-coordinate and all X would be bidentate, a cluster $Ti_2Zr_8O_8X_{24}$ would not be possible, because the number of ligands X is too small to fill all coordination sites. Similar considerations apply to $Ti_4Zr_4O_6(OBu)_4(OMc)_{16}$. Therefore, clusters with longer zigzag chains, based on the same construction principle as for the clusters shown in Fig. 10, cannot be expected.

The second series of Ti/Zr structures is based on an octahedral arrangement of the metal atoms in the monometallic clusters $Zr_6O_4(OH)_4(OOCR)_{12}$ (Zr_6O_8) and $Ti_6O_6(OR')_6(OOCR)_6$ (Ti_6O_6). Both were obtained for a variety of carboxylate ligands $RCOO^-$ (Fig. 11).

In the Zr_6O_8 clusters, the eight triangular faces of the M_6 octahedron are alternatively capped by μ_3-O or μ_3-OH groups. In contrast, only six triangular faces of the (distorted) Ti6 octahedron are capped by μ_3-O atoms in the Ti_6O_6 structures; two opposite faces are not capped. The reason for the different composition of the Zr_6O_8 and Ti_6O_6 clusters is the different coordination numbers of Ti (c.n. 6) and Zr (c.n. 8). While the total charge of M_6 is the same in both cases, the ligands in Zr_6O_8 must occupy 48 coordination sites, but only 36 in Ti_6O_6.

We recently isolated two Ti/Zr clusters, viz. $Ti_2Zr_4O_5(OH)_2(OPr)(OOCtBu)_{11}$ and $Ti_3Zr_3O_4(OH)_3(OBu)_3(OOCtBu)_{10}$, the structures of which are hybrids between that of Zr_6O_8 and Ti_6O_6 (Fig. 12) [36]. In the structure of the Ti_3Zr_3 cluster, half a Zr_6O_8 and half a Ti_6O_6 cluster are condensed which each other, i.e., one face of the Ti_3Zr_3 octahedron is occupied by the three Ti atoms and the opposite face by the three Zr atoms. The Zr_3 face and the

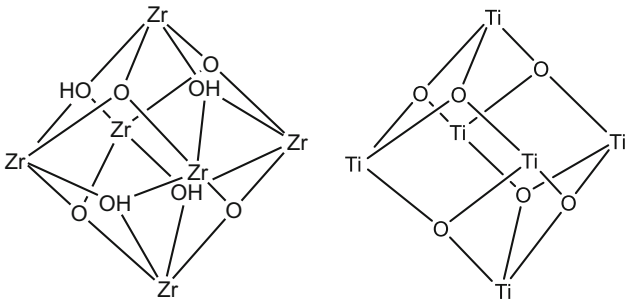

Fig. 11 Schematic drawing of the Zr_6O_8 core of $Zr_6O_4(OH)_4(OOCR)_{12}$ (*left*) and Ti_6O_6 core of $Ti_6O_6(OR)_6(OOCR')_6$ (*right*)

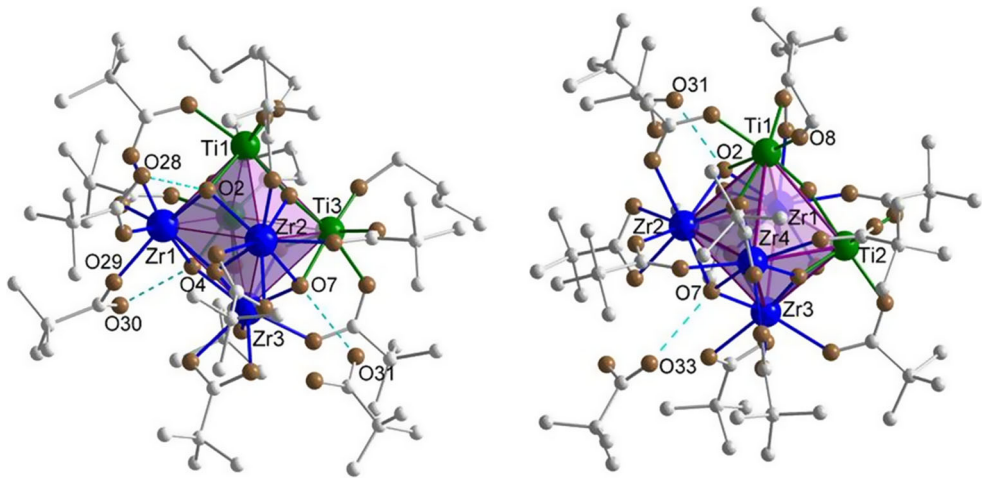

Fig. 12 Structures of $Ti_3Zr_3O_4(OH)_3(OBu)_3(OOCtBu)_{10}$ (*left*) and $Ti_2Zr_4O_5(OH)_2(OPr)(OOCtBu)_{11}$ (*right*) (from Ref. [36])

three $ZrTi_2$ faces are capped by μ_3-oxo groups, and the three Zr_2Ti faces by a μ_3-OH each. The Ti_3 face is not capped. The structure of the Ti_2Zr_4 cluster can be derived from that of Zr_6O_8 by replacing two neighboring Zr atoms by Ti. Because of the different coordination requirements of Ti, this results in a loss of a μ_3-O, as discussed for Ti_6O_6. The M_3 triangle not capped by an oxygen atom is that of the two Ti atoms and Zr4.

The titania–zirconia phase diagram [37] contains several ordered and disordered solid solutions of $(Zr,Ti)_2O_4$, the structures of which are not fully understood. Given the fact that the core of the Zr_6O_8 structures can be regarded as the smallest possible structural section of tetragonal zirconia which is stabilized by organic ligands, one can speculate that the cluster cores of $Ti_2Zr_4O_5(OH)_2(OPr)(OOCtBu)_{11}$ and $Ti_3Zr_3O_4(OH)_3(OBu)_3(OOCtBu)_{10}$ might be structurally related to structural motif(s) in tetragonal $(Zr,Ti)_2O_4$.

The alternative to using metal alkoxide mixtures for the preparation of mixed-metal oxides by sol–gel processing is the co-processing of a metal alkoxide and a metal salt (see one of the routes to Co_3O_4/CeO_2 composites above, as an example). The nature of the counter-ion will of course be another parameter that influences the obtained structures; therefore, we restricted ourselves to a series of acetates of di- and trivalent metals.

As was discussed before, an extension of the zigzag chain in the Ti/Zr structures is not possible with four-valent metals. When investigating reactions of titanium alkoxides with M(III) acetates and methacrylic acid, we found, however, that the central unit can be decorated by condensed polyhedra in different ways, depending on the ionic radii of the M^{3+} ions (Fig. 13) [38]. When the radius is small (Ln = Y [39], Sm, Eu, Gd, Ho, c.n. 8; 1.015–1.08 Å), the structures of the obtained oxo clusters $Ti_4Ln_2O_4(OMc)_{14}(HOMc)_2$ (Fig. 13, top) resemble very much that of $Ti_4Zr_2O_4(OBu)_6(OMc)_{10}$ (see Fig. 10). The only difference is the slightly different coordination of *two* $[TiO_6]$ octahedra terminating the chain of two $[TiO_6]$ and two $[MO_8]$ polyhedra. This is due to the different charge of the M^{3+} ion (and therefore two negatively charged ligands less). When the size of the M^{3+} ion is increased (Ln = Sm, Nd, Ce, La, c.n. 8; 1.08–1.16 Å), clusters $Ti_6Ln_2O_6(OMc)_{18}(HOiPr)$ are obtained in which the central unit of two $[TiO_6]$ and two $[MO_8]$ polyhedra is decorated by *four* additional $[TiO_6]$ octahedra (Fig. 13, center), apparently because there is more space available. For the biggest ions in this series (Ln = Ce, LN, c.n. 9; 1.20–1.22 Å), one central metal is sufficient to be condensed to four $[TiO_6]$ octahedra $[Ti_4LnO_3(OiPr)_2(OMc)_{11}$, Fig. 13, top]. Another way of looking at these structures is that the central ion polyhedron—depending on its size—is condensed to two, three or four $[TiO_6]$ octahedra and dimerized in the case of the smaller ions. Interestingly, a structure akin to that of the Ti_6Ln_2 was obtained upon reaction of $Ti(OiPr)_4$ with lead acetate and methacrylic acid. $Ti_6Pb_2O_5(OiPr)_4(OMc)_{14}$ differs in a way that the six $[TiO_6]$ units are arranged in a semicircle around the central M_2 unit rather than two opposite quarter-circles as in the Ti_6Ln_2 structure [40].

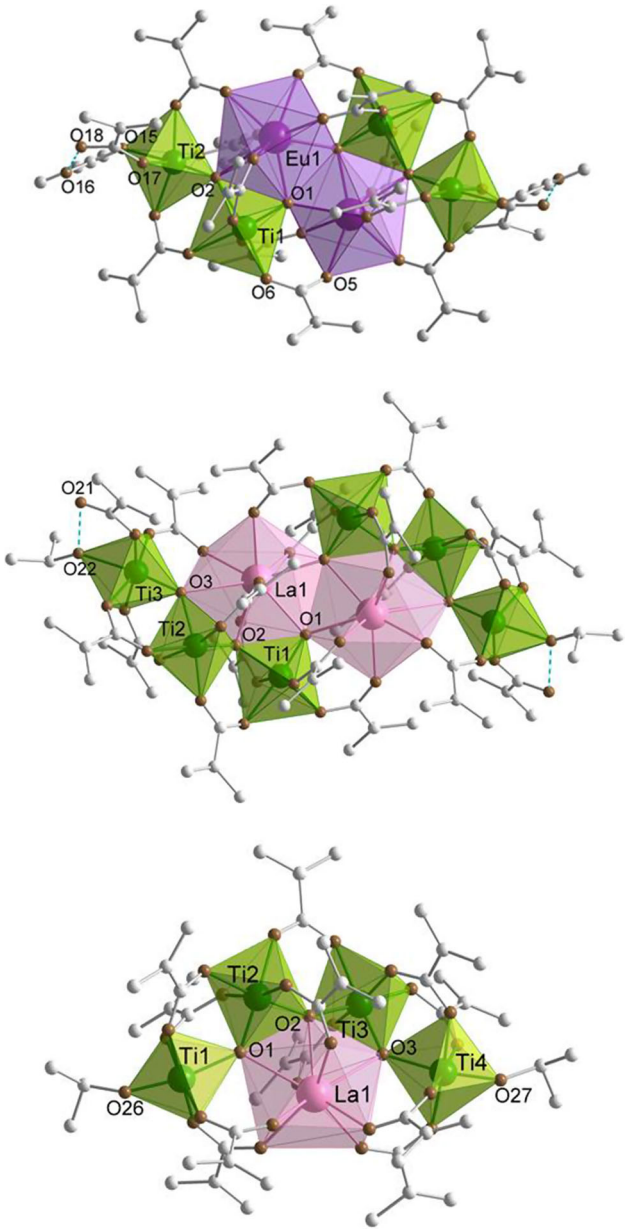

Fig. 13 Structures of $Ti_4Ln_2O_4(OMc)_{14}(HOMc)_2$ (*top*, Ln = Y, Sm, Eu, Gd, Ho, c.n. 8), $Ti_6Ln_2O_6(OMc)_{18}(HOiPr)$ (*center*, Ln = Sm, Nd, Ce, La, c.n. 8) and $Ti_4LnO_3(OiPr)_2(OMc)_{11}$ (*bottom*, Ln = La, Ce) (from Ref. [38])

Turning to M(II) ions, the mixed-metal oxo clusters $FeTi_5O_4(OiPr)_4(OMc)_{10}$, $Cd_4Ti_2O_2(OAc)_2(OMc)_{10}(HOiPr)_2$ (OAc = acetate), $Zn_2Ti_4O_4(OiPr)_2(OMc)_{10}$, $[Ca_2Ti_4O_4(OAc)_2(OMc)_{10}]_n$ and $[Sr_2Ti_4O_4(OMc)_{12}(HOMc)_2]_n$ were

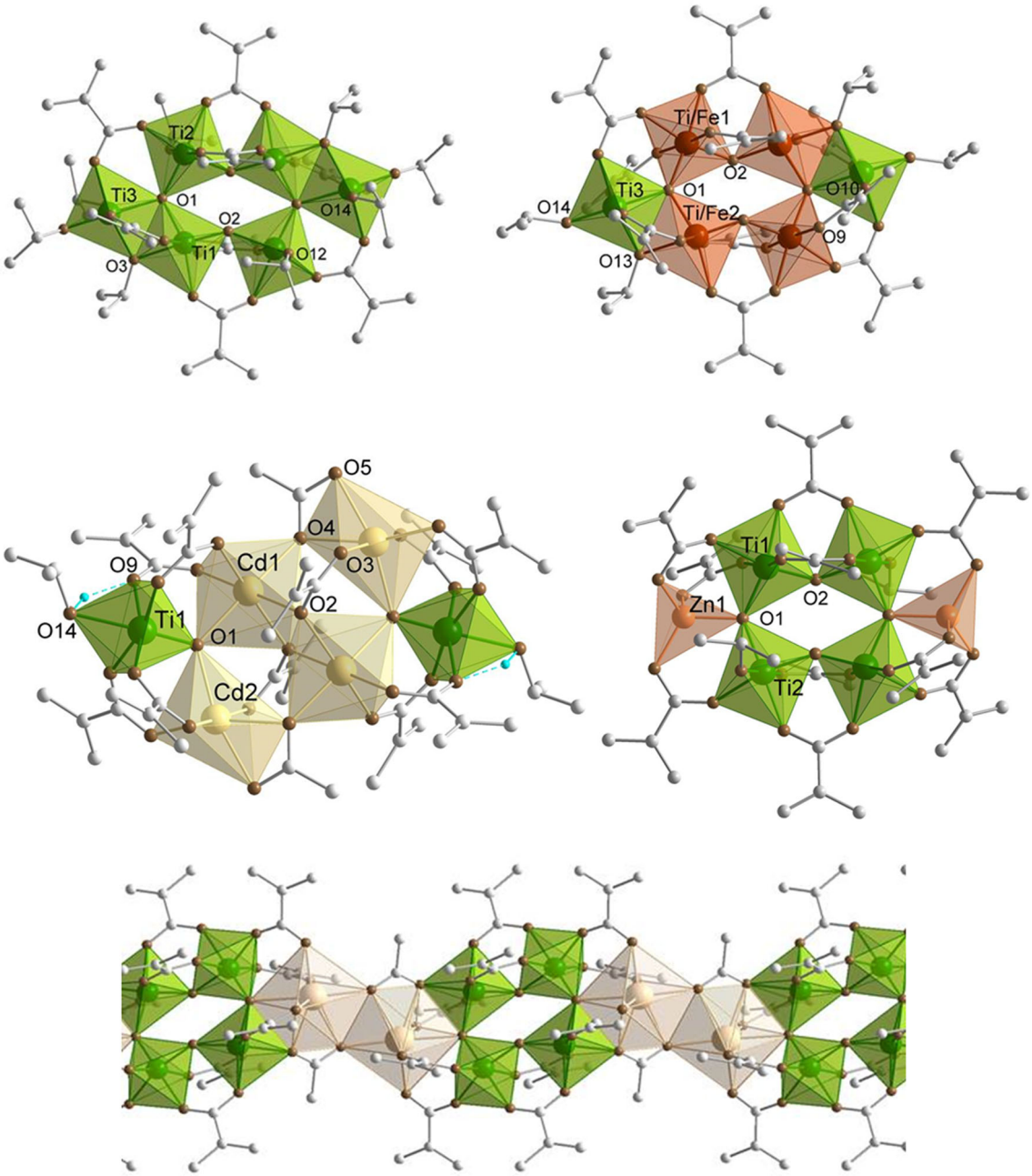

Fig. 14 Structures derived from $Ti_6O_4(OiPr)_8(OMc)_8$ (*top left*): $FeTi_5O_4(OiPr)_4(OMc)_{10}$ (*top right*), $Cd_4Ti_2O_2(OAc)_2(OMc)_{10}(HOiPr)_2$ (*center left*), $Zn_2Ti_4O_4(OiPr)_2(OMc)_{10}$ (*center right*) and $[Ca_2Ti_4O_4(OAc)_2(OMc)_{10}]_n$ (*bottom*) (from Ref. [41])

obtained from the reaction of titanium alkoxides with the corresponding metal acetates and methacrylic acid (Fig. 14) [41]. Their structures are derived from those of monometallic clusters with the composition $Ti_6O_4(OR)_8(OOCR')_8$ for which various R/R′ combinations are known [21]. Quite surprisingly, the general structure is retained when part of the Ti atoms is replaced by two-valent atoms (Fe^{2+}, Zn^{2+}, Cd^{2+}, Ca^{2+}, Sr^{2+}). The lower charge and different coordination numbers of the second metal, however, render modification of the ligand sphere necessary.

Fe^{2+} and Ti^{4+} have similar bonding characteristics with oxygen and the ionic radii are almost equal (0.61 and 0.605 Å), and hence one of the four inner Ti^{4+} sites is replaced by Fe^{2+} in $FeTi_5O_4(OiPr)_4(OMc)_{10}$. In contrast, the ionic radius of Cd^{2+} is much bigger (0.95 Å). This results in replacement of the inner Ti atoms by Cd in

$Cd_4Ti_2O_2(OAc)_2(OMc)_{10}(HO\mathit{i}Pr)_2$. Both Fe and Cd are octahedrally coordinated like Ti, and the lower charge, however, is compensated by a different coordination behavior of a smaller number of ligands. Zn^{2+} has the same size as Fe^{2+} and Ti^{4+}, but is tetrahedrally coordinated. In $Zn_2Ti_4O_4(O\mathit{i}Pr)_2(OMc)_{10}$, the two outer Ti octahedra of the Ti_6 reference structure are replaced by Zn tetrahedra, with corresponding adjustment of the connecting ligands. Ca^{2+} and Sr^{2+} ions are much bigger and have higher coordination numbers, and the bonds are less directed. In the Ca and Sr compounds, the outer Ti octahedra of the Ti_6 reference structure are substituted with Ca or Sr polyhedra. Different to the Fe, Cd and Zn derivatives where molecular clusters were obtained, the Ca and Sr derivatives form chains of condensed clusters in the crystal lattice.

The fact that very much related structures are formed with a given set of ligands, despite considerably different ionic radii and coordination numbers of the metals, shows that the M_6O_4 structural motif is very robust and tolerant to a major variation.

4 Conclusions

Mixed-metal systems add another challenging dimension to sol–gel science. It is a trivial fact in sol–gel science that every additional component in the precursor mixture increases the complexity of the system considerably. This is especially true for a second metal component because it can participate in the network-forming processes. The golden thread of this article is the relative positioning of the two metals, one of the key issues in bimetallic systems.

In the first part of this article, a SSP approach was discussed by which two network-forming elements (silicon and a metal, or two metals) are interconnected through a hydrolytically stable organic linker. This approach is relatively easy for Si because of the availability or easy accessibility of organotrialkoxysilanes $(RO)_3Si(CH_2)_nX$, in which the group X can coordinate to metal ions, metal alkoxide moieties, etc. SSPs $[(RO)_3Si–Y–X]_nM$ are therefore easily obtained. Formation of SSPs with any combination of two metals is more difficult, because it requires bifunctional organic compounds X′–Y–X with two different coordinating groups (X and X′) where each of them must selectively react with just one metal to give SSPs of the type M′(X′–Y–X)M. Although less straightforward than for Si/M combinations and requiring some chemical expertise, it was shown in this article that this approach is feasible and results in an excellent control over the dispersion of the two metals in the final bimetallic oxides. This approach has hardly been exploited until present. It must be stressed that both $[(RO)_3Si–Y–X]_nM$ and M′(X′–Y–X)M can be formed in situ, i.e., must not be isolated, before sol–gel processing. Removal of the organic groups from the gels is usually by heat treatment in air, i.e., by burning the organic groups. This initially generates porous solids with high surface areas.

The starting point of the second part of this article was the notion that molecular oxo clusters, obtained by incomplete hydrolysis and condensation of metal compounds, might be snapshots of the development of structural units in gels. An unexpected feature of our investigation of Ti/M bimetallic oxo clusters was the finding that a high percentage of them can be traced back to a few basic structures. Furthermore, bimetallic clusters were formed in nearly all cases, and in only very few cases, monometallic clusters were isolated. It must be emphasized, however, that all our systems contained carboxylate ligands (either from the added acid or from metal acetate precursors) which bridged the two metals. These findings make us confident to believe that the oxo clusters are indeed model compounds and that key features of their structures, especially the interlinked metals, can be extrapolated to gel structures.

Acknowledgments I thank all coworkers and collaborators who, during many years, participated in this work for their outstanding contributions. Their names are mentioned in the references. Recent work was financially supported by the *Fonds zur Förderung der wissenschaftlichen Forschung*, Wien.

References

1. Brinker CJ, Scherer GW (1990) Sol–gel science: the physics, chemistry of sol–gel processing. Academic Press, San Diego
2. Vioux A (1997) Chem Mater 9:2292 **(Review article)**
3. Veith M (2002) Dalton Trans 2405 **(Review article)**
4. Singh A, Mehrotra RC (2004) Coord Chem Rev 248:101 **(Review article)**
5. Schubert U, Amberg-Schwab S, Breitscheidel B (1989) Chem Mater 1:576
6. Breitscheidel B, Zieder J, Schubert U (1991) Chem Mater 3:559
7. Lembacher C, Schubert U (1998) New J Chem 22:721
8. Urbaniak W, Schubert U (1991) Liebigs Ann Chem 1221
9. Broudic JC, Conocar O, Moreau JJE, Meyer D, Wong-Chi-Man M (1999) J Mater Chem 9:2283
10. Feinle A, Flaig S, Puchberger M, Schubert U, Hüsing N (2015) Chem Commun 51:2339
11. Trimmel G, Schubert U (2001) J Non-Cryst Solids 296:188
12. Deshmukh R, Schubert U (2011) J Mater Chem 21:18534
13. Deshmukh R (2012) PhD thesis, TU Wien
14. Felbermair E, Sidorenko A, Paschen S, Akbarzadeh J, Peterlik H, Schubert U (2014) Chem Eur J 20:9212
15. Fric H, Schubert U (2005) New J Chem 29:232

16. Fric H, Puchberger M, Schubert U (2006) J Sol-Gel Sci Technol 40:155
17. Schubert U (2007) Acc Chem Res 40:730
18. Rupp W, Hüsing N, Schubert U (2002) J Mater Chem 12:2594
19. Torma V, Peterlik H, Bauer U, Rupp W, Hüsing N, Bernstorff S, Steinhart M, Goerigk G, Schubert U (2005) Chem Mater 17:3146
20. Peterlik H, Rennhofer H, Torma V, Bauer U, Puchberger M, Hüsing N, Bernstorff S, Schubert U (2007) J Non-Cryst Solids 353:1635
21. Schubert U (2005) J Mater Chem 15:3701 **(Review article)**
22. Yang J, Puchberger M, Qian R, Maurer C, Schubert U (2012) Eur J Inorg Chem 4294
23. Yang J, Akbarzadeh J, Maurer C, Peterlik H, Schubert U (2012) J Mater Chem 22:24034
24. Yang J, Lukashuk L, Akbarzadeh J, Stöger-Pollach M, Peterlik H, Föttinger K, Rupprechter G, Schubert U (2015) Chem Eur J 21:885
25. Wang J, Shen M, Wang J, Gao J, Ma J, Liu S (2011) Catal Today 175:65
26. Klemperer WG, Mainz VV, Ramamurthi SD, Rosenberg FS (1988) Better ceramics through chemistry III. Materilas Research Society, Pittsburgh
27. Brown JF (1965) J Am Chem Soc 87:4317
28. Piana K, Schubert U (1994) Chem Mater 6:1504
29. Day VW, Eberspacher TA, Chen Y, Hao J, Klemperer WG (1995) Inorg Chim Acta 229:391
30. Campana CF, Chen Y, Day VW, Klemperer WG, Sparks RA (1996) J Chem Soc Dalton Trans 691
31. Hubert-Pfalzgraf LG (2003) Inorg Chem Commun 6:102
32. Hubert-Pfalzgraf LG (2004) J Mater Chem 14:3113
33. Schubert U (2001) Chem Mater 13:3487 **(Review article)**
34. Moraru B, Kickelbick G, Schubert U (2001) Eur J Inorg Chem 1295
35. Gross S, Kickelbick G, Puchberger M, Schubert U (2003) Monatsh Chem 134:1053
36. Artner C, Czakler M, Schubert U (2015) Inorg Chim Acta 432:208
37. Troitzsch U, Ellis DJ (2005) J Mater Sci 40:4571
38. Artner C, Kronister S, Czakler M, Schubert U (2014) Eur J Inorg Chem 5596
39. Jupa M, Kickelbick G, Schubert U (2004) Eur J Inorg Chem 1835
40. Artner C, Czakler M, Schubert U (2014) Chem Eur J 20:493
41. Artner C, Koyun A, Czakler M, Schubert U (2014) Eur J Inorg Chem 5008